Journal of Microbiology (2021) Vol. 59, No. 12, pp. 1133–1141
DOI 10.1007/s12275-021-1518-5
eISSN 1976-3794
pISSN 1225-8873

Regulator of ribonuclease activity modulates the pathogenicity of *Vibrio vulnificus*

Jaejin Lee[1†], Eunkyoung Shin[1†], Jaeyeong Park[1], Minho Lee[2*], and Kangseok Lee[1*]

[1]*Department of Life Science, Chung-Ang University, Seoul 06974, Republic of Korea*
[2]*Department of Microbiology, College of Medicine, Hallym University, Chuncheon 24252, Republic of Korea*

(Received Oct 5, 2021 / Revised Oct 19, 2021 / Accepted Oct 20, 2021)

RraA, a protein regulator of RNase E activity, plays a unique role in modulating the mRNA abundance in *Escherichia coli*. The marine pathogenic bacterium *Vibrio vulnificus* also possesses homologs of RNase E (VvRNase E) and RraA (VvRraA1 and VvRraA2). However, their physiological roles have not yet been investigated. In this study, we demonstrated that VvRraA1 expression levels affect the pathogenicity of *V. vulnificus*. Compared to the wild-type strain, the *VvrraA1*-deleted strain (Δ*VvrraA1*) showed decreased motility, invasiveness, biofilm formation ability as well as virulence in mice; these phenotypic changes of Δ*VvrraA1* were restored by the exogenous expression of *VvrraA1*. Transcriptomic analysis indicated that VvRraA1 expression levels affect the abundance of a large number of mRNA species. Among them, the half-lives of mRNA species encoding virulence factors (e.g., *smcR* and *htpG*) that have been previously shown to affect *VvrraA1* expression-dependent phenotypes were positively correlated with *VvrraA1* expression levels. These findings suggest that VvRraA1 modulates the pathogenicity of *V. vulnificus* by regulating the abundance of a subset of mRNA species.

Keywords: RNase E, VvRraA1, virulence, pathogenicity, *Vibrio vulnificus*

Introduction

Vibrio vulnificus is a Gram-negative marine bacterium that causes fulminant primary septicemia in humans at risk of infection, and has a high rate of morbidity and mortality (Li *et al.*, 2019; López-Pérez *et al.*, 2019). Three pathological biotypes of *V. vulnificus* exist; biotype 1 is the most common and elicits all symptoms of illness, including primary sepsis. *V. vulnificus* MO6-24/O is a highly virulent strain belonging to biotype 1. Biotype 2 strains usually infect eels, and rarely infect humans (Raz *et al.*, 2014; Oliver, 2015; Li *et al.*, 2019), whereas biotype 3, which is a hybrid of biotypes 1 and 2, can cause severe disease in humans, with a mortality rate of ~8% (Ziolo *et al.*, 2014). Various factors, including extracellular hemolysin (VvhA), metalloprotease (VvpE), RtxA1 exotoxin, and lipopolysaccharide (LPS), have been suggested as determinants of virulence in *V. vulnificus* (Jones and Oliver, 2009; Li and Wang, 2020).

In several pathogenic bacteria, RNase E has been implicated in the control of virulence-related gene expression (Lee *et al.*, 2021). For instance, depletion of RNase E was linked to decreased *stx2*, which encodes the Shiga toxin, a major virulence factor in *E. coli* O157:H7 (Thuraisamy and Lodato, 2018). In *Yersinia* spp., RNase E is considered a positive regulator of genes encoding the type III secretion system (Yang *et al.*, 2008). Moreover, coordination of full-length RNase E with small regulatory RNAs (sRNAs) is required for the virulence of *Brucella abortus* (Sheehan *et al.*, 2020). RNase E is a highly conserved protein with several interaction partners in γ-proteobacteria (Aït-Bara *et al.*, 2015; Lee *et al.*, 2021; Moore *et al.*, 2021), and RraA has been shown to regulate RNase E activity (Lee *et al.*, 2003, 2009, 2011; Heo *et al.*, 2016; Kim *et al.*, 2016; Seo *et al.*, 2017). *Vibrio vulnificus* has an ortholog of RNase E and RraA, designated VvRNase E and VvRraA1 and VvRraA2, respectively, and their conserved roles in cleaving representative substrates for RNase E have been shown (Lee *et al.*, 2009, 2011; Kim *et al.*, 2016; Song *et al.*, 2017). However, the role of RraA in RNase E-mediated pathogenicity has not yet been elucidated. In this study, we investigated the involvement of *VvrraA1* in the pathogenicity of *V. vulnificus*.

Materials and Methods

Animals

Mouse feeding and experimental procedures were performed as previously described (Yeom *et al.*, 2016; Song *et al.*, 2019). Pathogen-free 6-week-old female BALB/c mice (n = 10) were purchased from Saeron Bio.

Ethical statement

All animal experiments were performed in accordance with the National Guidelines for the Use of Animals in Scientific Research and were approved by the Chung-Ang University Support Center (Approval No. CAU2012-0044).

Bacterial and eukaryotic strains

The bacterial strains, plasmids, and oligonucleotides used in this study are listed in Tables 1 and 2. *Vibrio vulnificus*

†These authors contributed equally to this work.
*For correspondence. (K. Lee) E-mail: kangseok@cau.ac.kr; Tel.: +82-2-820-5241; Fax: +82-2-825-5206 / (M. Lee) E-mail: mlee@hallym.ac.kr; Tel.: +82-33-248-2633

Table 1. List of strains and plasmids used in this study

Strains	Description	References
Vibrio vulnificus		
MO6-24/O	Clinical isolate	Wright *et al.* (1990)
Δ*VvrraA1*	MO6-24/O but Δ*VvrraA1*	This study
Escherichia coli		
DH5α	*supE44* D*lacU169* (f80 *lacZ* DM15) *hsdR1 recA1 endA1 gyrA96 thi-1 relA1*	Laboratory strain
SM10λpir	*thi-1 thr leu tonA lacY supE* recA::Rp4-2Tc::Mu λ*pir*, Km^R	Simon *et al.* (1983)
Plasmids	**Description**	**References**
pRK415	RK2-derived *oriV*, Tc^R	Keen *et al.* (1988)
pRK415-VvrraA1	pRK415 containing the promoter and CDS of *VvrraA1*	This study
pUC4K	pUC4 with *nptI*; Amp^R, Km^R	Pharmacia Biotech
pDM4	Suicide vector; *ori* R6K, Cm^R	Milton *et al.* (1996)
pDM4-5′UTR	pDM4 containing the 5′ UTR of *VvrraA1*	This study
pDM4-5′-3′UTR	pDM4 containing the 5′ and 3′ UTR of *VvraA1*	This study
pDM4-VvrraA1	pDM4 containing the 5′ UTR and 3′ UTR of *VvrraA1* and *nptI* gene	This study

MO6-24/O strains (WT, Δ*VvrraA1*, and Δ*VvrraA1*^{comple}) were grown at 30°C in Luria-Bertani medium (Becton, Dickinson and Company) supplemented with 1.9% NaCl (LBS), or AB medium supplemented with 1% sodium succinate (Kim *et al.*, 2009). *E. coli* DH5α and SM10λpir were used for plasmid cloning and conjugation into *V. vulnificus* strains, respectively. Antibiotics were added at the following concentrations: 2 μg/ml tetracycline (Tc) and 50 μg/ml kanamycin (Km). The cervical cancer (HeLa) cell line was cultured in Dulbecco's modified Eagle's medium (DMEM; Welgene) containing 10% heat-inactivated fetal bovine serum (FBS; Welgene) and 1% penicillin-streptomycin (PS; Welgene) at 37°C in an incubator with a 5% CO_2 humidified atmosphere.

Construction of the *VvrraA1*-expressing plasmid and *VvrraA1*-deletion mutant

Complementation of *VvrraA1* was prepared by molecular cloning into pRK415 with the 5′ UTR containing its native promoter, coding sequence, and 3′ UTR of *VvrraA1*. To construct pRK415-VvrraA1, *VvrraA1* was amplified using polymerase chain reaction (PCR) using the primers VvrraA1-PstI (F) and VvrraA1-*Xba*I (R), and subsequently digested with *Pst*I and *Bam*HI. The fragment was ligated into pRK415 using 250 units of T4 DNA ligase (TaKaRa). The *VvrraA1*-deletion mutant was constructed using the homologous recombination method (Blomfield *et al.*, 1991). The 5′ and 3′ UTRs of *VvrraA1* were amplified using VvrraA1 5′-UTR (F)/VvrraA1 5′-UTR (R) for the 5′ UTR, and VvrraA1 3′-UTR (F)/VvrraA1 3′-UTR (R) for the 3′ UTR. Genomic DNA of *V. vulnificus* MO6-24/O was used as the template. The Km^R gene (*nptI* gene) was digested using *Bam*HI from pUC4K. The resulting fragments were digested with *Apa*I, *Bam*HI, and *Sac*I (TaKaRa), and subsequently cloned into pDM4. The suicide vector containing the deletion cassette was conjugated into *V. vulnificus* MO6-24/O, in which allelic homologous recombination occurred.

Table 2. Oligonucleotides used in this study

Oligonucleotides	Sequences
For gene cloning	
VvrraA-PstI-F	5′-TTCTGCAGCGGTGGCGCCTTAATGGCCTTT-3′
VvrraA-XbaI-R	5′-AATCTAGATTAATCGAGCAGCTCTGGCTCT-3′
For gene knockout	
VvrraA1 5′-UTR-F	5′-GGGCCCCCGTGAAAGGAACTGATAAC-3′
VvrraA1 5′-UTR-R	5′-GGATCCGGCATACCTTCTTTGGTCAA-3′
VvrraA1 3′-UTR-F	5′-GGATCCAGAGAAAAAAGCGTCACTTT-3′
VvrraA1 3′-UTR-R	5′-GAGCTCAAATCGAAGGAAGAGTAAAA-3′
For qRT-PCR	
V-qR-rpsG-F	5′-ACACTATGGCTGAGAAATCTGG-3′
V-qR-rpsG-R	5′-GGACGTACTTCTACTGGAACTTG-3′
V-qR-smcR-F	5′-GTTTGGCCTCTGTTTGTCAC-3′
V-qR-smcR-R	5′-GTTGGTACGGTTTGCTTGAAC-3′
V-qR-luxS-F	5′-TTCACACGTTAGAGCACCTG-3′
V-qR-luxS-R	5′-CACTTTCAACACATCTTCCATCG-3′
V-qR-htpG-F	5′-CCATCTTACTTGCGTTTTGTCC-3′
V-qR-htpG-R	5′-CGTAGCGATTGAGTCACCTTG-3′
V-qR-ompU-F	5′-ACGGTGTTGGTTTCTACGAAG-3′
V-qR-ompU-R	5′-GTCACTTCACCAAACTTGCC-3′

Western blot analysis

Western blot analysis was performed as previously described (Lee *et al.*, 2019). *Vibrio vulnificus* strains were harvested at an OD_{600} of 3, washed once with 1 × phosphate buffered saline (PBS), and resuspended in 25 μl of 1 × PBS and 2 × SDS loading dye. Cell lysates were denatured at 95°C for 15 min. Subsequently, 2–3 μl of the lysate was loaded onto a 15% sodium dodecyl sulfate (SDS) polyacrylamide gel and transferred onto a 0.2 μm nitrocellulose membrane (Amersham Bioscience). Membranes were incubated overnight with polyclonal antibodies against RraA (1:1,000) and S1 (1:20,000) at 4°C, followed by 3 h incubation with goat anti-mouse antibody (1:10,000) (Enzo Biochem) at 25°C. Detection was performed using Luminol reagent (Santa Cruz Biotechnology). Relative protein abundance was quantified using Quantity One software (Bio-Rad).

Total RNA sequencing

Vibrio vulnificus Δ*VvrraA1* harboring pRK415 and *V. vulnificus* Δ*VvrraA1* harboring pRK415-VvrraA1 were grown at 30°C in LBS medium containing Tc (2 μg/ml) to an OD_{600} of 3. Total RNA was extracted using the Purelink RNA kit

(Invitrogen). RNA sequencing was performed by Macrogen on a NovaSeq 6000 platform using 200-bp paired-end read sequencing. The preceding workflow used is as follows: Ribosomal RNA in total RNA was removed using a Ribo-Zero rRNA removal kit (Illumina), and a TruSeq Stranded Total RNA Sample Prep Kit (Illumina) was used for library construction (Whon *et al.*, 2021).

RNA-seq data analysis

Paired-end reads were aligned with the genomic DNA reference of *V. vulnificus* (GCF_000186585.1_Aspof.V1) using Bowtie aligner (Na, 2020). The differentially expressed genes were determined using the edgeR software package to have a raw p-value < 0.05, and |fold change| ≥ 1.4. The raw p-value for RNA-seq was generated using a modified Fisher's exact test. Raw data are available at https://www.ncbi.nlm.nih.gov/sra/PRJNA739628.

Real-time quantitative reverse transcription PCR (qRT-PCR)

Total RNA was extracted from WT, *VvrraA1*-deleted (Δ*VvrraA1*), and complemented (Δ*VvrraA1*^{comple}) at an OD_{600} of 3 using a Purelink RNA kit (Invitrogen). cDNA was synthesized from 250 ng of total RNA using a PrimeScript 1st strand cDNA synthesis kit (TaKaRa) (Park *et al.*, 2020). qRT-PCR was performed with 5-fold diluted cDNA of each strain containing iQ SYBR Green supermix (Bio-Rad) in a CFX-96 thermal cycler (Bio-Rad).

Measurement of mRNA stability

Vibrio vulnificus strains were cultured overnight in LBS medium at 30°C, diluted in fresh LBS medium, and further incubated at 30°C to an OD_{600} of 3. To stop RNA transcription, rifampicin (Sigma-Aldrich) was added to the cultures at a final concentration of 1 mg/ml. To measure the half-life of *smcR* and *htpG* mRNA, the culture samples were collected 1, 2, 4, and 8 min after rifampicin treatment, and total RNA preparation and qRT-PCR were performed as described above.

Measurement of lengths of cells and flagella

The lengths of cells and flagella were determined using images captured at 80 kV using a transmission electron microscope (TEM) (JEOL). *Vibrio vulnificus* strains (WT, Δ*VvrraA1*, and Δ*VvrraA1*^{comple}) were cultured on LBS agar plates. Following this, the bacterial cells were washed twice with distilled water and transferred onto formvar grids. The cells were then stained with 1% phosphotungstic acid (Han and Lee, 2020). The length of cells (n = 60) and flagella (n = 50) were determined using ImageJ software (NIH).

Motility test using semi-solid agar

Vibrio vulnificus strains (WT, Δ*VvrraA1*, and Δ*VvrraA1*^{comple}) were grown at 30°C in LBS medium containing Tc (1 μg/ml) to an OD_{600} of 3. Subsequently, 5 μl of cells were spotted onto semi-solid LBS agar (LBS, 0.3% Bacto agar; Becton, Dickinson and Company). The spotted plates were incubated for 18 h at 30°C, and the motility diameter was measured (Kim and Ko, 2020). Three independent experiments were performed in triplicate.

Motility test via live cell imaging

Vibrio vulnificus strains (WT, Δ*VvrraA1*, and Δ*VvrraA1*^{comple}) were grown at 30°C in LBS medium to the late log phase (OD_{600} = 3.0). Samples were prepared by diluting the cell suspension 100-fold with fresh medium, followed by spotting 3 μl of each strain onto microscope slides and placing a covering glass (Paul Marienfeld GmbH & Co. KG). The motility of single cells was observed using a Nikon DS Qi2 camera connected to a Nikon Eclipse Ti microscope (Nikon), with a Nikon 100 × 1.40 NA Plan Apo VC oil-immersion objective lens (Nikon), and visualized using Nikon NIS-Elements software. The average instantaneous velocity of a single cell was measured every 0.07 sec for 1 sec (duplicated, n = 22).

Biofilm formation assay

Vibrio vulnificus strains cultured overnight (WT, Δ*VvrraA1*, and Δ*VvrraA1*^{comple}) were incubated to an OD_{600} of 0.5, with AB-succinate medium (Kim *et al.*, 2009) supplemented with Tc (2 μg/ml), and then diluted 10-fold, followed by incubation for 40 h at 30°C in borosilicate tubes in a static state. The planktonic cells were removed using 1 × PBS and stained with 1% crystal violet for 30 min (Jung *et al.*, 2019). The biofilms were washed with distilled water and dried at room temperature. Biofilms solubilized in 100% ethanol were quantified at 550 nm using spectrophotometry.

Growth curve

Pre-cultured *V. vulnificus* strains (WT, Δ*VvrraA1*, and Δ*VvrraA1*^{comple}) were inoculated at 100-fold into fresh LBS medium supplemented with Tc (1 μg/ml) and incubated for 8 h at 240 rpm. Growth curves were measured in triplicate.

Gentamicin protection assay

HeLa cells were seeded at a density of 5×10^4 cells/well in 24-well culture dishes. After 24 h, the host cells were infected with *V. vulnificus* for 20 min at a multiplicity of infection (MOI) of 20. Infected HeLa cells were washed five times with 1 × PBS, and non-intracellular bacterial cells were removed using free DMEM containing gentamicin (50 μg/ml). Infected HeLa cells were lysed in 1 × PBS containing 2% NaCl and 1% Triton X-100 for 5 min. The number of invading bacteria was calculated by counting colony-forming units (CFUs) (Zhi *et al.*, 2019).

Lactate dehydrogenase assay

HeLa cells were seeded at a density of 1×10^4 cells/well. After the existing DMEM was replaced with free DMEM, HeLa cells were incubated with *V. vulnificus* at an MOI of 20 for 1, 2, 3, and 4 h. Supernatants were collected to measure the amount of lactate dehydrogenase released from HeLa cells. The Cytotox 96 non-radioactive cytotoxicity kit (Promega) was used according to the manufacturer's instructions.

Mouse experiments

Vibrio vulnificus grown to the log phase were diluted using 1 × PBS to 5×10^5 cells/ml, and 5×10^4 CFU were intraperitoneally inoculated (n = 10) into iron-dextran-treated mice.

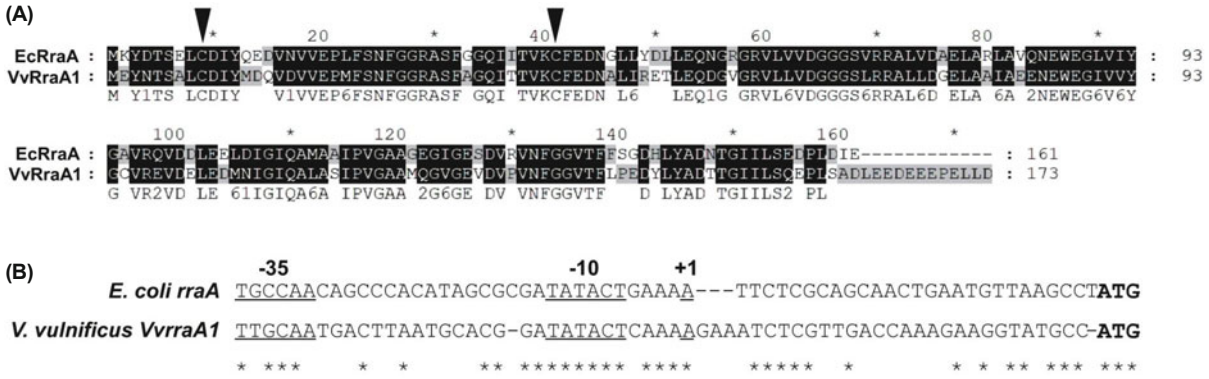

Fig. 1. Sequence analysis of *VvrraA1*. (A) Protein sequence analysis of VvRraA1 and EcRraA. The protein sequence was obtained from the UniProt database, aligned using ClustalW, and visualized using GeneDoc software. Black background represents identical residues, whereas white or gray backgrounds indicate dissimilar residues. The numbers below the sequence alignment are Similarity scores in amino acids sequences. Conserved Cys9 and Cys41 residues of RraA proteins are highlighted by arrows. (B) Promoter analysis of *VvrraA1* and *EcrraA*. Nucleotide sequences show the promoter regions of *VvrraA1* and *EcrraA* genes. The promoter regions for -35, -10, and transcription start site (+1) are underlined.

Quantification and statistical analyses

Student's *t*-test was used for comparisons with controls, using SigmaPlot (Systat Software, Inc.). Data are presented as the mean ± SEM, and p-value < 0.05 was considered to indicate statistical significance. All statistical details of the experiments are included in the figure legends.

Results

VvRraA1 levels are growth phase-dependent

RraA proteins are widely distributed in prokaryotes such as archaea and γ-proteobacteria (Monzingo *et al.*, 2003). Previous studies have shown that RraA homologs of *V. vulnificus* (VvRraA1 and VvRraA2) have high protein sequence similarity (80% and 59%, respectively), and that VvRraA1 can efficiently inhibit VvRNase E activity (Kim *et al.*, 2016; Song *et al.*, 2017). Both VvRraA1 and EcRraA contain Cys9 and Cys41, which are involved in the hexameric assembly of the RraA homolog (Fig. 1A) (Song *et al.*, 2017). In addition, *VvrraA1* has a conserved promoter region similar to that of *EcrraA*, which is regulated by a stationary-phase sigma factor σ^S at the transcription level (Zhao *et al.*, 2006) (Fig. 1B). To investigate whether *VvrraA1* expression is controlled by σ^S, the relative expression level of *VvrraA1* was measured in *V. vulnificus* cells during their growth phases. In contrast to EcRraA, VvRraA1 expression levels gradually increased from the early log to the late log phase and decreased in the stationary phase of growth (Fig. 2A), indicating that growth-dependent *VvrraA1* expression might be different from that of *EcrraA*. Based on these results, we considered the transition from the log phase to the stationary phase, a time when VvRraA1 protein is highly expressed, as a good time points to observe inhibition of RNase E activity and changes in physiological activity by VvRraA1 in *V. vulnificus*.

To determine whether VvRraA1 expression influences the pathogenicity of *V. vulnificus*, *VvrraA1*-deleted (Δ*VvrraA1*) and complemented (Δ*VvrraA1*^{comple}) strains were constructed, and VvRraA1 levels were measured using western blot analysis (Fig. 2B). We observed that the Δ*VvrraA1*^{comple} strain expressed approximately six times more VvRraA1 compared to the WT strain, whereas VvRraA1 expression was not detected in the Δ*VvrraA1* strain. In addition, the Δ*VvrraA1*^{comple} strain showed a moderately slower growth rate compared to the WT and Δ*VvrraA1* strains (Fig. 2C).

VvRraA1 positively regulates the pathogenicity of *V. vulnificus*

Biofilm formation is considered a critical stage in the pathogenesis of many bacterial species (Costerton *et al.*, 1999; Donlan, 2001; Gulig *et al.*, 2005). To investigate whether *VvrraA1* expression influences biofilm formation, the VvrraA1-expression dependent biofilm-forming ability of *V. vulnificus* was measured. The degree of biofilm formation decreased by ~35% in the Δ*VvrraA1* strain, whereas it increased by ~35% in the Δ*VvrraA1*^{comple} strain, compared to that in the WT strain (Fig. 3A). To further investigate the effects of VvRraA1 levels on pathogenicity, several other parameters were evaluated. To assess VvRraA1 level-dependent invasiveness of *V. vulnificus* cells in host cells, a gentamicin protection assay was performed using HeLa cells. The results showed that the number of invading Δ*VvrraA1* cells was 12% lower than that of WT cells, whereas the Δ*VvrraA1*^{comple} strain showed ~5 times higher number of invading cells compared to that of the WT strain (Fig. 3B). Next, the cytotoxicity assay, which measures the lactate dehydrogenase released from host cells, was performed and the results showed no dramatic changes in the number of viable HeLa cells when the WT and Δ*VvrraA1* strains were used. Approximately 40% more HeLa cells survived when Δ*VvrraA1*^{comple} cells were infected at prolonged infection times (Fig. 3C). This result is likely to stem from a moderately slower growth rate of the Δ*VvrraA1*^{comple} strain compared to that of the WT and Δ*VvrraA1* strains (Fig. 2C). To further test whether changes in *in vitro* invasion and cytotoxicity of these strains affect *in vivo* virulence, the WT and Δ*VvrraA1* strains were allowed to infect BALB/c mice. The results showed that mice infected with Δ*VvrraA1* survived for a significantly longer time compared to those infected with WT cells (Fig. 3D). These results suggest that

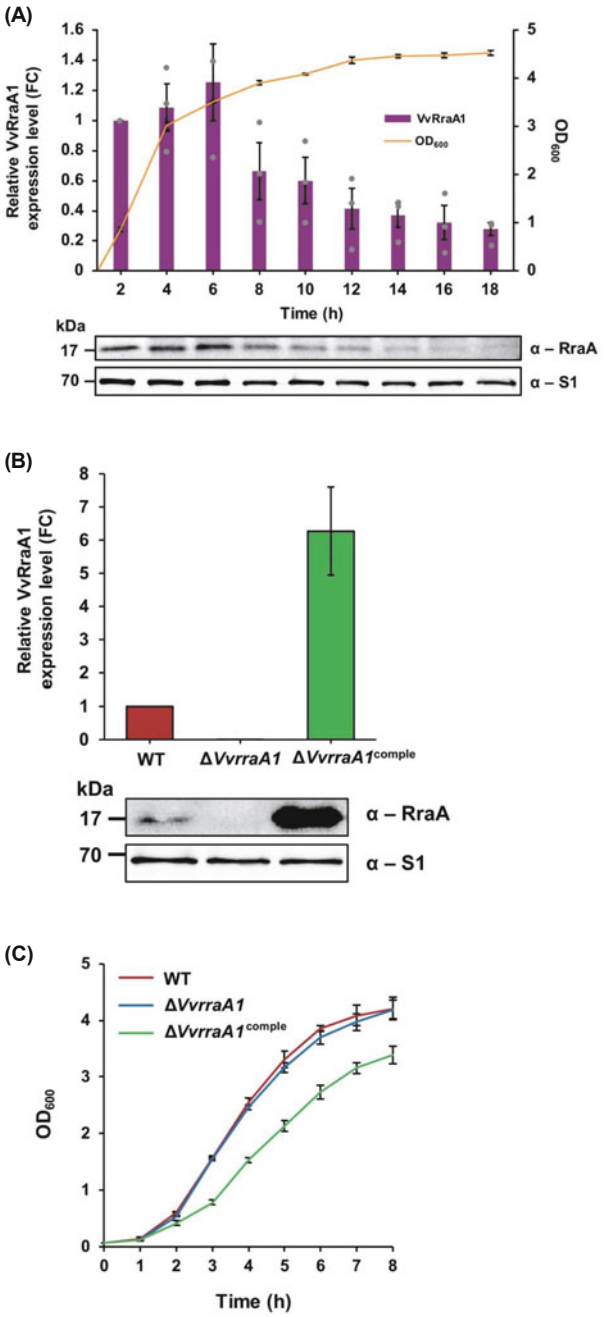

Fig. 2. Expression levels of VvRraA1. (A) The expression level of VvRraA1 protein in WT cells. The expression level of VvRraA1 in the WT strain. Total lysates were prepared from the indicated time and analyzed using western blotting to determine the abundance of VvRraA1 protein. Quantification of VvRraA1 protein in WT cells was normalized to samples harvested at 2 h, using Quantity One software. Data represent the mean ± SEM of three independent experiments. (B) VvRraA1 expression levels in WT, Δ*VvrraA1*, and Δ*VvrraA1*^{comple}. Total cell lysates were prepared after 4 h of incubation at 30°C. The abundance of VvRraA1 was normalized using WT strain. Polyclonal antibodies against RraA and S1 were used. The data are representative of two independent experiments. (C) Growth characteristics of the WT, Δ*VvrraA1*, and Δ*VvrraA1*^{comple} strains. The strains were grown in LBS medium and optical density at 600 nm (OD_{600}) was measured every hour (h) at 30°C in a shaking incubator (240 rpm). Three independent experiments were performed in triplicates. Error bars represent mean ± SEM. For (A) and (B), ribosomal protein S1 was used as an internal standard.

VvRraA1 levels influence the pathogenicity level in *V. vulnificus*.

VvRraA1 levels affect the swimming motility, flagella length, and cell size

To investigate how VvRraA1 levels influence the pathogenicity of *V. vulnificus*, swimming motility was measured using soft agar and single-cell tracking assays (Fig. 4A and B). The motility on soft agar decreased by ~20% in the Δ*VvrraA1* strain compared to that in the WT strain (Fig. 4A). The motility of Δ*VvrraA1* cells, measured by single cell tracking assay, decreased by 17% compared to that of Δ*VvrraA1*^{comple} cells (Fig. 4B). To further determine whether the decreased motility was a consequence of changes in flagella length, the length of flagella was measured by analyzing TEM images. As shown in Fig. 4C, flagellar length increased by 0.42 μm when *VvrraA1* was exogenously expressed in Δ*VvrraA1* cells, although it was not significantly different in WT and Δ*VvrraA1* cells. In addition, the length of Δ*VvrraA1* cells decreased compared to that of WT cells and was restored to the WT length in Δ*VvrraA1*^{comple} cells (Fig. 4D). These results suggest that VvRraA1 levels affect the motility and morphological characteristics of *V. vulnificus*.

VvRraA1 levels affect the mRNA abundance of a subset of genes in *V. vulnificus*

To investigate whether VvRraA1 expression-dependent changes in pathogenicity are related to VvRraA1-mediated regulation of mRNA abundance, RNA sequencing (RNA-seq) was performed using total RNA extracted from the *VvrraA1*-deleted (Δ*VvrraA1*) and complemented (Δ*VvrraA1*^{comple}) strains. When differentially expressed genes (DEGs) of the Δ*VvrraA1* strain versus the Δ*VvrraA1*^{comple} strain were analyzed, of the 4,400 genes detected by RNA sequencing, the mRNA abundance of ~3,000 genes was found to vary at least 1.4-fold, with significant differences (Fig. 5A). The mRNA abundance of 1,563 genes showed an increase in the Δ*VvrraA1* strain, whereas 1,402 genes showed lower mRNA abundance compared to that in the Δ*VvrraA1*^{comple} strain (Fig. 5A). These results suggest that VvRraA1 overexpression widely influences the transcriptomic profile, similar to EcRraA (Lee *et al.*, 2003). Based on the RNA-seq data, four mRNAs, whose expression levels decreased in the Δ*VvrraA1* strain compared to those in the Δ*VvrraA1*^{comple} strain, were chosen for further investigation because they are known to play important roles in the pathogenicity of *V. vulnificus*. These mRNAs encode the quorum-sensing system LuxS/SmcR, chaperone protein HtpG, and outer membrane protein OmpU (Fig. 5B). These factors are associated with many virulence processes, including host cell invasion, biofilm formation, and cytotoxicity. To verify the RNA-seq data, qRT-PCR was performed using total RNA isolated from WT, Δ*VvrraA1,* and Δ*VvrraA1*^{comple} cells. The results showed that the mRNA abundance of *smcR* and *htpG* was lower in Δ*VvrraA1* cells than in Δ*VvrraA1*^{comple} cells, which is consistent with the RNA-seq data (Fig. 5C). However, no significant changes were observed in the relative abundance of *luxS* and *ompU* mRNAs in these strains (Fig. 5C).

Next, to determine whether VvRraA1 levels affect the sta-

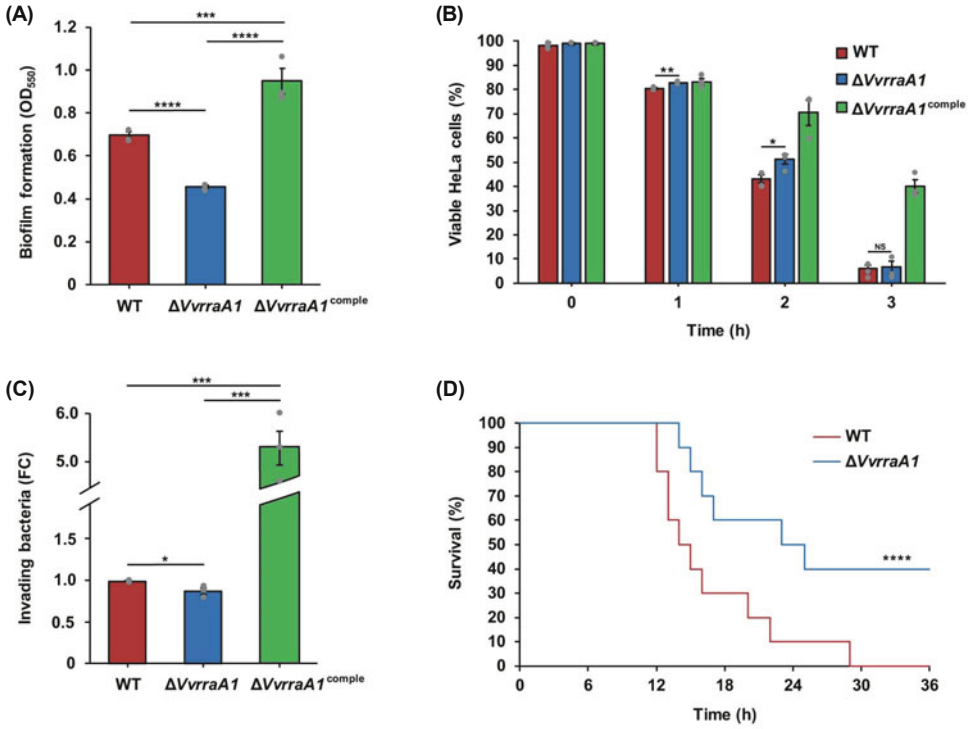

Fig. 3. Effects of VvRraA1 levels on the pathogenicity of *V. vulnificus*. (A) Effects of VvRraA1 levels on biofilm formation. The *V. vulnificus* strains (WT, Δ*VvrraA1*, and Δ*VvrraA1*^{comple}) were grown to an OD_{600} of 3, inoculated into borosilicate tubes containing LBS supplemented with tetracycline (2 μg/ml), and incubated for 40 h at 30°C. (B) The human cervical carcinoma cells were used for evaluating invasion. HeLa cells (1×10^5 cells/well) were infected with *V. vulnificus* strains (WT, Δ*VvrraA1*, and Δ*VvrraA1*^{comple}) for 20 min at a multiplicity of infection (MOI) of 20. Non-intracellular bacteria were removed by treatment with gentamicin (50 μg/ml). The infected host cells were lysed with treatment of 1 × PBS containing 1.9% NaCl and 1% Triton X-100 for 5 min, and the concentration of bacteria that infected the host cells was determined by analyzing the number of colony forming units (CFU). (C) HeLa cells were infected with *V. vulnificus* strains (WT, Δ*VvrraA1*, and Δ*VvrraA1*^{comple}) at MOI of 1:20. Cell viability was determined by measuring the lactate dehydrogenase released from the host cells. (D) Mouse mortality test was performed using BALB/c female mouse. Ten mice were infected intraperitoneally with 10^4 CFU of WT and Δ*VvrraA1* strains. For (A), (B), (C), and (D), the data are presented as the mean ± SEM of three independent experiments. The significant differences were generated using two-sided unpaired Student's *t*-test. $^*p < 0.05$, $^{**}p < 0.01$, $^{***}p < 0.001$, and $^{****}p < 0.0001$.

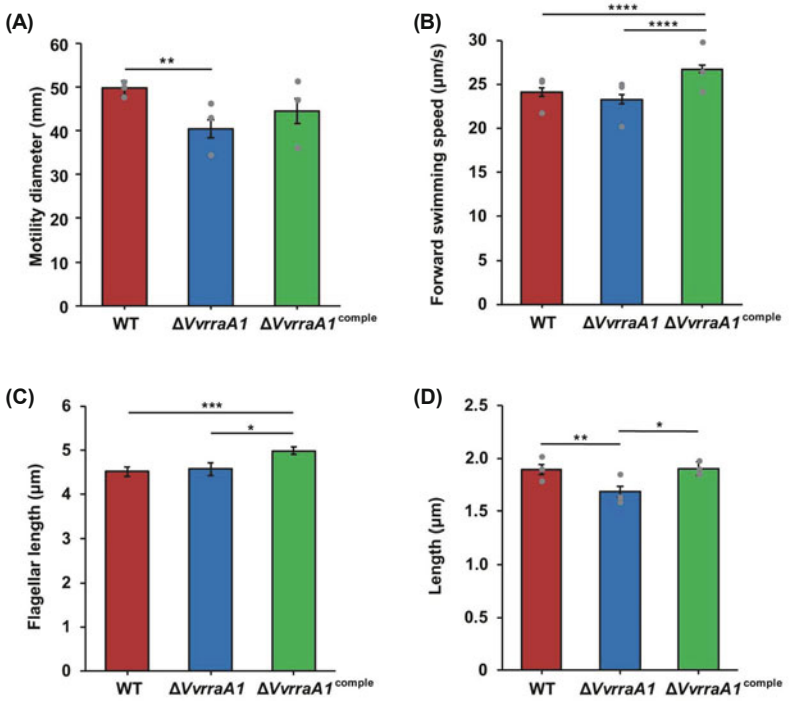

Fig. 4. Effects of VvRraA1 levels on the motility, flagella length, and cell size of *V. vulnificus*. (A and B) Effect of VvRraA1 levels on the motility. (A) Swimming diameter was determined by spotting onto LBS agar plates containing 0.3% Bacto agar. Five milliliters of cells cultured to the late-log phase were inoculated and incubated for 6 h at 30°C. (B) Single cells were visualized at 1,000 × magnification, and the average speed of single cells was measured based on the instantaneous velocity of bacterium every 0.07 sec for 1 sec (duplicated, $n = 22$). For (A) and (B), the data are presented as the mean ± SEM of three independent experiments. The asterisk indicates statistically significant differences (two-sided unpaired Student's *t*-test, $^{**}p < 0.01$ and $^{****}p < 0.0001$). (C and D) Effect of VvRraA1 levels on the morphological characteristics. (C) Effects of VvRraA1 on the flagella length. TEM images were prepared by negative staining at 10,000 × magnification. Error bars represent ± SEM ($n = 50$). (D) Effects of VvRraA1 on the cell size. Error bars indicate ± SEM ($n = 60$). ImageJ software was used for measuring the length of flagella and cells. For (C) and (D), the significance of differences was obtained by two-sided unpaired Student's *t*-test. $^*p < 0.05$, $^{**}p < 0.01$, and $^{***}p < 0.001$. For (A), (B), (C), and (D), WT harboring pRK415, Δ*VvrraA1* harboring pRK415, and Δ*VvrraA1*^{comple} harboring pRK415-VvrraA1 were prepared at an OD_{600} of 3 in LBS medium containing tetracycline (2 μg/ml).

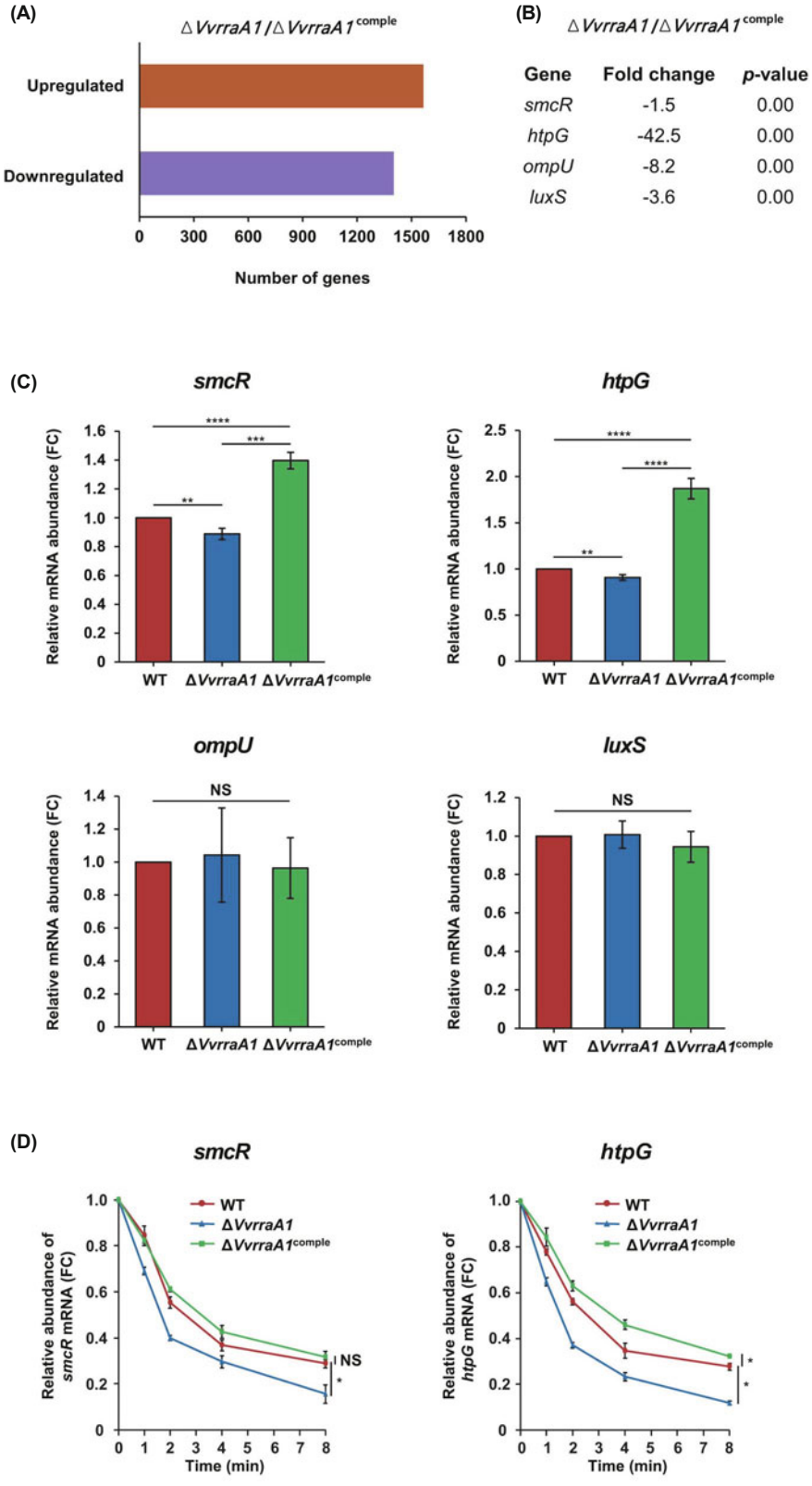

Fig. 5. Identification of mRNA species whose abundance is associated with VvRraA1 levels. (A) Genes whose abundance is regulated by VvRraA1. VvRraA1-regulated genes were assessed using RNA-sequencing analysis (Δ*VvrraA1* strain vs. Δ*VvrraA1*^{comple} strain). The group of genes had a fold-change (FC) value of > 1.4, and a *p*-value < 0.5. The 1,563 upregulated genes are on the upper side, and the 1,402 downregulated genes are at the bottom. (B) Four genes whose abundance is regulated by VvRraA1 were obtained based on RNA-seq data, with a fold change of > 1.4, and a *p*-value < 0.05. (C) The relative expression of genes was analyzed using the $2^{-\Delta\Delta Ct}$ method with *rpsG* as the reference gene. The data are presented as the mean ± SEM of three independent experiments. Asterisks represent significant differences (two-sided unpaired Student's *t*-test). $^{**}p < 0.01$, $^{***}p < 0.001$, and $^{****}p < 0.0001$. NS, no significance. (D) Effects of VvRraA1 on *smcR* and *htpG* mRNAs stability in the *V. vulnificus* cultures used in (C) measured using qRT-PCR. *smcR* and *htpG* mRNAs expression was normalized using *rpsG* mRNA, and gene expression was quantified using the $2^{-\Delta\Delta Ct}$ method. The data are presented as the mean ± SEM of three independent experiments. Asterisks represent significant differences (two-sided unpaired Student's *t*-test). $^{*}p < 0.05$, and NS, no significance.

bility of *smcR* and *htpG* mRNAs, we measured the half-lives of these mRNAs in the WT, Δ*VvrraA1*, and Δ*VvrraA1*^{comple} strains using quantitative RT-PCR. The results showed that the half-life of *smcR* mRNA was ~1.6- and 2-fold higher in the WT and Δ*VvrraA1*^{comple} cells (2 min 50 sec and 3 min 30 sec, respectively) than in the Δ*VvrraA1* cells (1 min 45 sec)

(Fig. 5D). We observed analogous results when the half-lives of *htpG* mRNA were measured (2 min 55 sec, 3 min 55 sec, and 1 min 50 sec in the WT, Δ*VvrraA1*^{comple}, and Δ*VvrraA1* strains, respectively). These results indicate that VvRraA1 levels positively affect the stability of *smcR* and *htpG* mRNA.

Discussion

In this study, we showed that VvRraA1 levels affect virulence-related processes, including motility, biofilm formation, and *in vivo* and *in vitro* pathogenicity of *V. vulnificus* (Figs. 3 and 4). The complementation of *VvrraA1* in the Δ*VvrraA1*^{comple} strain showed retarded growth, a significant increase in the invasive ability, and reduced toxicity in host cells compared to the WT strain.

RNA-seq and qRT-PCR analyses showed a correlation between VvRraA1 levels and the abundance of two mRNAs encoding the quorum sensing regulator SmcR and the heat shock protein HtpG (Fig. 5). We postulate that this observation is likely to be associated with VvRraA1 level-dependent phenotypic alterations in *V. vulnificus* for the following reasons. First, in *V. vulnificus*, deletion of *smcR* resulted in decreased biofilm formation, motility, cytotoxicity, and virulence in mice (Kim *et al.*, 2003, 2013a, 2013b; Lee *et al.*, 2007). Second, *htpG* mutants exhibited decreased biofilm-forming ability in *V. vulnificus* and *P. aeruginosa* (Kim *et al.*, 2007; Grudniak *et al.*, 2018). Third, it has been shown that the expression of *flhF*, encoding an essential protein for flagella synthesis, is affected by SmcR (Kim *et al.*, 2012). Finally, an *htpG*-deleted *Pseudomonas aeruginosa* mutant exhibited significantly diminished motility (Grudniak *et al.*, 2018).

However, we do not have direct evidence showing that VvRraA1 level-dependent phenotypic alterations in *V. vulnificus* were a consequence of the inhibition of VvRNase E-mediated cleavage of *smcR* and *htpG* mRNAs by VvRraA1. Considering that the half-life and mRNA abundance of *htpG* are increased in *E. coli rne-1* mutants (Perwez and Kushner, 2006; Stead *et al.*, 2011), it is likely that the *htpG* mRNA abundance is controlled by VvRraA1-dependent modulation of VvRNase E activity. Further studies are needed to unveil the VvRraA1-dependent modulation of VvRNase E activity on *smcR* and *htpG* mRNA.

As RraA overexpression leads to pleiotropic phenotypes in *E. coli* because of the increased abundance of mRNAs, which are RNase E-targeted substrates (Lee *et al.*, 2003), *VvrraA1* expression-dependent changes in the abundance of other mRNAs encoding virulence factors, in addition to *smcR* and *htpG*, may also contribute to the pathogenicity of *V. vulnificus*.

In conclusion, our present study indicates the involvement of RraA proteins in the pathogenicity of bacterial species.

Acknowledgements

This research was supported by the Chung-Ang University Graduate Research Scholarship in 2020 and the National Research Foundation of Korea (grant no. NRF- 2021R1A2-C3008934 to K. L.).

Conflict of Interest

The authors have declared that no competing interests exist.

Ethical Statements

All animal experiments were performed in accordance with the National Guidelines for the Use of Animals in Scientific Research and were approved by the Chung-Ang University Support Center (Approval No. CAU2012-0044).

References

Aït-Bara, S., Carpousis, A.J., and Quentin, Y. 2015. RNase E in the γ-Proteobacteria: conservation of intrinsically disordered noncatalytic region and molecular evolution of microdomains. *Mol. Genet. Genomics* **290**, 847–862.

Blomfield, I.C., Vaughn, V., Rest, R.F., and Eisenstein, B.I. 1991. Allelic exchange in *Escherichia coli* using the *Bacillus subtilis sacB* gene and a temperature-sensitive pSC101 replicon. *Mol. Microbiol.* **5**, 1447–1457.

Costerton, J.W., Stewart, P.S., and Greenberg, E.P. 1999. Bacterial biofilms: a common cause of persistent infections. *Science* **284**, 1318–1322.

Donlan, R.M. 2001. Biofilm formation: a clinically relevant microbiological process. *Clin. Infect. Dis.* **33**, 1387–1392.

Grudniak, A.M., Klecha, B., and Wolska, K.I. 2018. Effects of null mutation of the heat-shock gene *htpG* on the production of virulence factors by *Pseudomonas aeruginosa*. *Future Microbiol.* **13**, 69–80.

Gulig, P.A., Bourdage, K.L., and Starks, A.M. 2005. Molecular pathogenesis of *Vibrio vulnificus*. *J. Microbiol.* **43**, 118–131.

Han, Y. and Lee, E.J. 2020. Detecting *Salmonella* type II flagella production by transmission electron microscopy and immunocytochemistry. *J. Microbiol.* **58**, 245–251.

Heo, J., Kim, D., Joo, M., Lee, B., Seo, S., Lee, J., Song, S., Yeom, J.H., Ha, N.C., and Lee, K. 2016. RraAS2 requires both scaffold domains of RNase ES for high-affinity binding and inhibitory action on the ribonucleolytic activity. *J. Microbiol.* **54**, 660–666.

Jones, M.K. and Oliver, J.D. 2009. *Vibrio vulnificus*: disease and pathogenesis. *Infect. Immun.* **77**, 1723–1733.

Jung, S., Park, O.J., Kim, A.R., Ahn, K.B., Lee, D., Kum, K.Y., Yun, C.H., and Han, S.H. 2019. Lipoteichoic acids of lactobacilli inhibit *Enterococcus faecalis* biofilm formation and disrupt the preformed biofilm. *J. Microbiol.* **57**, 310–315.

Keen, N.T., Tamaki, S., Kobayashi, D., and Trollinger, D. 1988. Improved broad-host-range plasmids for DNA cloning in Gram-negative bacteria. *Gene* **70**, 191–197.

Kim, D., Kim, Y.H., Jang, J., Yeom, J.H., Jun, J.W., Hyun, S., and Lee, K. 2016. Functional analysis of *Vibrio vulnificus* orthologs of *Escherichia coli* RraA and RNase E. *Curr. Microbiol.* **72**, 716–722.

Kim, S.Y. and Ko, K.S. 2020. Cryptic prophages in a *bla*$_{NDM-1}$-bearing plasmid increase bacterial survival against high NaCl concentration, high and low temperatures, and oxidative and immunological stressors. *J. Microbiol.* **58**, 483–488.

Kim, S.M., Lee, D.H., and Choi, S.H. 2012. Evidence that the *Vibrio vulnificus* flagellar regulator FlhF is regulated by a quorum sensing master regulator SmcR. *Microbiology* **158**, 2017–2025.

Kim, H.S., Lee, M.A., Chun, S.J., Park, S.J., and Lee, K.H. 2007. Role of NtrC in biofilm formation via controlling expression of the gene encoding an ADP-*glycero*-*manno*-heptose-6-epimerase in the pathogenic bacterium, *Vibrio vulnificus*. *Mol. Microbiol.* **63**, 559–574.

Kim, S.Y., Lee, S.E., Kim, Y.R., Kim, C.M., Ryu, P.Y., Choy, H.E., Chung, S.S., and Rhee, J.H. 2003. Regulation of *Vibrio vulnificus* virulence by the LuxS quorum-sensing system. *Mol. Microbiol.* **48**, 1647–1664.

Kim, H.S., Park, S.J., and Lee, K.H. 2009. Role of NtrC-regulated exopolysaccharides in the biofilm formation and pathogenic interaction of *Vibrio vulnificus*. *Mol. Microbiol.* **74**, 436–453.

Kim, S.M., Park, J.H., Lee, H.S., Kim, W.B., Ryu, J.M., Han, H.J., and Choi, S.H. 2013a. LuxR homologue SmcR is essential for *Vibrio vulnificus* pathogenesis and biofilm detachment, and its expression is induced by host cells. *Infect. Immun.* **81**, 3721–3730.

Kim, I.H., Wen, Y., Son, J.S., Lee, K.H., and Kim, K.S. 2013b. The *fur*-iron complex modulates expression of the quorum-sensing master regulator, SmcR, to control expression of virulence factors in *Vibrio vulnificus*. *Infect. Immun.* **81**, 2888–2898.

Lee, J., Lee, D.H., Jeon, C.O., and Lee, K. 2019. RNase G controls *tpiA* mRNA abundance in response to oxygen availability in *Escherichia coli*. *J. Microbiol.* **57**, 910–917.

Lee, J.H., Rhee, J.E., Park, U., Ju, H.M., Lee, B.C., Kim, T.S., Jeong, H.S., and Choi, S.H. 2007. Identification and functional analysis of *Vibrio vulnificus* SmcR, a novel global regulator. *J. Microbiol. Biotechnol.* **17**, 325–334.

Lee, M., Ryu, M., Joo, M., Seo, Y.J., Lee, J., Kim, H.M., Shin, E., Yeom, J.H., Kim, Y.H., Bae, J., *et al.* 2021. Endoribonuclease-mediated control of *hns* mRNA stability constitutes a key regulatory pathway for *Salmonella* Typhimurium pathogenicity island 1 expression. *PLoS Pathog.* **17**, e1009263.

Lee, M., Yeom, J.H., Jeon, C.O., and Lee, K. 2011. Studies on a *Vibrio vulnificus* functional ortholog of *Escherichia coli* RNase E imply a conserved function of RNase E-like enzymes in bacteria. *Curr. Microbiol.* **62**, 861–865.

Lee, M., Yeom, J.H., Sim, S.H., Ahn, S., and Lee, K. 2009. Effects of *Escherichia coli* RraA orthologs of *Vibrio vulnificus* on the ribonucleolytic activity of RNase E *in vivo*. *Curr. Microbiol.* **58**, 349–353.

Lee, K., Zhan, X., Gao, J., Qiu, J., Feng, Y., Meganathan, R., Cohen, S.N., and Georgiou, G. 2003. RraA: a protein inhibitor of RNase E activity that globally modulates RNA abundance in *E. coli*. *Cell* **114**, 623–634.

Li, G. and Wang, M.Y. 2020. The role of *Vibrio vulnificus* virulence factors and regulators in its infection-induced sepsis. *Folia Microbiol.* **65**, 265–274.

Li, X., Zhou, Y., Jiang, Q., Yang, H., Pi, D., Liu, X., Gao, X., Chen, N., and Zhang, X. 2019. Virulence properties of *Vibrio vulnificus* isolated from diseased zoea of freshness shrimp *Macrobrachium rosenbergii*. *Microb. Pathog.* **127**, 166–171.

López-Pérez, M., Jayakumar, J.M., Haro-Moreno, J.M., Zaragoza-Solas, A., Reddi, G., Rodriguez-Valera, F., Shapiro, O.H., Alam, M., and Almagro-Moreno, S. 2019. Evolutionary model of cluster divergence of the emergent marine pathogen *Vibrio vulnificus*: from genotype to ecotype. *mBio* **10**, e02852-18.

Milton, D.L., O'Toole, R., Horstedt, P., and Wolf-Watz, H. 1996. Flagellin A is essential for the virulence of *Vibrio anguillarum*. *J. Bacteriol.* **178**, 1310–1319.

Monzingo, A.F., Gao, J., Qiu, J., Georgiou, G., and Robertus, J.D. 2003. The X-ray structure of *Escherichia coli* RraA (MenG), A protein inhibitor of RNA processing. *J. Mol. Biol.* **332**, 1015–1024.

Moore, C.J., Go, H., Shin, E., Ha, H.J., Song, S., Ha, N.C., Kim, Y.H., Cohen, S.N., and Lee, K. 2021. Substrate-dependent effects of quaternary structure on RNase E activity. *Genes Dev.* **35**, 286–299.

Na, D. 2020. User guides for biologists to learn computational methods. *J. Microbiol.* **58**, 173–175.

Oliver, J.D. 2015. The biology of *Vibrio vulnificus*. *Microbiol. Spectr.* **3**, 3.3.01.

Park, S.J., Lim, S., and Choi, J.I. 2020. Improved tolerance of *Escherichia coli* to oxidative stress by expressing putative response regulator homologs from Antarctic bacteria. *J. Microbiol.* **58**, 131–141.

Perwez, T. and Kushner, S.R. 2006. RNase Z in *Escherichia coli* plays a significant role in mRNA decay. *Mol. Microbiol.* **60**, 723–737.

Raz, N., Danin-Poleg, Y., Hayman, R.B., Bar-On, Y., Linetsky, A., Shmoish, M., Sanjuán, E., Amaro, C., Walt, D.R., and Kashi, Y. 2014. Genome-wide SNP-genotyping array to study the evolution of the human pathogen *Vibrio vulnificus* biotype 3. *PLoS ONE* **9**, e114576.

Seo, S., Kim, D., Song, W., Heo, J., Joo, M., Lim, Y., Yeom, J.H., and Lee, K. 2017. RraAS1 inhibits the ribonucleolytic activity of RNase ES by interacting with its catalytic domain in *Streptomyces coelicolor*. *J. Microbiol.* **55**, 37–43.

Sheehan, L.M., Budnick, J.A., Fyffe-Blair, J., King, K.A., Settlage, R.E., and Caswell, C.C. 2020. The endoribonuclease RNase E coordinates expression of mRNAs and small regulatory RNAs and is critical for the virulence of *Brucella abortus*. *J. Bacteriol.* **202**, e00240-20.

Simon, R., Priefer, U., and Pühler, A. 1983. A broad host range mobilization system for *in vivo* genetic engineering: transposon mutagenesis in Gram negative bacteria. *Nat. Biotechnol.* **1**, 784–791.

Song, S., Hong, S., Jang, J., Yeom, J.H., Park, N., Lee, J., Lim, Y., Jeon, J.Y., Choi, H.K., Lee, M., *et al.* 2017. Functional implications of hexameric assembly of RraA proteins from *Vibrio vulnificus*. *PLoS ONE* **12**, e0190064.

Song, W., Joo, M., Yeom, J.H., Shin, E., Lee, M., Choi, H.K., Hwang, J., Kim, Y.I., Seo, R., Lee, J.E., *et al.* 2019. Divergent rRNAs as regulators of gene expression at the ribosome level. *Nat. Microbiol.* **4**, 515–526.

Stead, M.B., Marshburn, S., Mohanty, B.K., Mitra, J., Pena Castillo, L., Ray, D., van Bakel, H., Hughes, T.R., and Kushner, S.R. 2011. Analysis of *Escherichia coli* RNase E and RNase III activity *in vivo* using tiling microarrays. *Nucleic Acids Res.* **39**, 3188–3203.

Thuraisamy, T. and Lodato, P.B. 2018. Influence of RNase E deficiency on the production of *stx2*-bearing phages and Shiga toxin in an RNase E-inducible strain of enterohaemorrhagic *Escherichia coli* (EHEC) O157:H7. *J. Med. Microbiol.* **67**, 724–732.

Whon, T.W., Shin, N.R., Kim, J.Y., and Roh, S.W. 2021. Omics in gut microbiome analysis. *J. Microbiol.* **59**, 292–297.

Wright, A.C., Simpson, L.M., Oliver, J.D., and Morris, J.G.Jr. 1990. Phenotypic evaluation of acapsular transposon mutants of *Vibrio vulnificus*. *Infect. Immun.* **58**, 1769–1773.

Yang, J., Jain, C., and Schesser, K. 2008. RNase E regulates the *Yersinia* type 3 secretion system. *J. Bacteriol.* **190**, 3774–3778.

Yeom, J.H., Lee, B., Kim, D., Lee, J.K., Kim, S., Bae, J., Park, Y., and Lee, K. 2016. Gold nanoparticle-DNA aptamer conjugate-assisted delivery of antimicrobial peptide effectively eliminates intracellular *Salmonella enterica* serovar Typhimurium. *Biomaterials* **104**, 43–51.

Zhao, M., Zhou, L., Kawarasaki, Y., and Georgiou, G. 2006. Regulation of RraA, a protein inhibitor of RNase E-mediated RNA decay. *J. Bacteriol.* **188**, 3257–3263.

Zhi, Y., Lin, S.M., Jang, A.Y., Ahn, K.B., Ji, H.J., Guo, H.C., Lim, S., and Seo, H.S. 2019. Effective mucosal live attenuated *Salmonella* vaccine by deleting phosphotransferase system component genes *ptsI* and *crr*. *J. Microbiol.* **57**, 64–73.

Ziolo, K.J., Jeong, H.G., Kwak, J.S., Yang, S., Lavker, R.M., and Satchell, K.J. 2014. *Vibrio vulnificus* biotype 3 multifunctional autoprocessing RTX toxin is an adenylate cyclase toxin essential for virulence in mice. *Infect. Immun.* **82**, 2148–2157.